Hindawi
Geofluids
Volume 2018, Article ID 8459289, 7 pages
https://doi.org/10.1155/2018/8459289

WILEY | Hindawi

Research Article

Groundwater Level Distribution in Vacuum Dewatering Method in Phreatic Aquifer

Feng Huang, Jianguo Lyu, He Gao, and Zhaoteng Yu

School of Engineering & Technology, China University of Geosciences, Beijing 100083, China

Correspondence should be addressed to Jianguo Lyu; ljg@cugb.edu.cn

Received 15 December 2017; Revised 6 February 2018; Accepted 13 February 2018; Published 14 March 2018

Academic Editor: Marco Petitta

Vacuum dewatering method has been widely used in geotechnical engineering. However, there is little research on the groundwater level distribution under the effect of vacuum pressure which is generated by vacuum wells. In view of this, the groundwater level distribution in phreatic aquifer is analyzed. First, the vacuum pressure distribution in soil is analyzed through Darcy's law and steady-state seepage control equation based on established particles and pores model. Second, the boundary conditions are modified by the vacuum pressure distribution law and then the water level distribution equations in flow boundary and waterhead boundary conditions are derived. Finally, dewatering experiment is carried out to analyze the water levels in vacuum and nonvacuum dewatering and verify the theoretical model of water level distribution in vacuum dewatering. The results show that, in both boundary conditions, the water levels in vacuum dewatering are lower than those in nonvacuum dewatering. The theoretical values agree with the experimental values well, which proves the rationality of theoretical equations and predicting the water levels in vacuum dewatering method.

1. Introduction

Groundwater has brought great difficulties and risks to underground engineering, especially in fractured aquifer [1–5]. Engineering accidents occur frequently due to improper groundwater treatment. Therefore, effective groundwater treatment is an important subject of engineering safety. Among groundwater control methods, dewatering has been widely used in slope treatment and large underground engineering. Nowadays, dewatering method mainly includes large diameter well, radial well, electroosmosis well, light well point, and vacuum tube well. Peila et al. [6] and Bianco and Bruce [7] discussed the use of large diameter wells in landslide stabilization. Large diameter (up to 2 m) wells are drilled vertically and each well is connected to its neighbour by a horizontal drill hole. Thus, all water attracted and intercepted by these large drainage columns is transmitted by gravity to a convenient draw off point. This system has been used to depths of over 50 m [7]. A radial well includes the main well and horizontal wells. The main well is drilled vertically, which is connected to several horizontal wells. Then, the water seeps into the main well through the horizontal wells. Huang et al. [8] analyzed the solution of transient drawdown for constant-flux pumping at a partially penetrating well in a radial two-zone confined aquifer and Dimkic et al. [9] discussed the simulation method of the radial wells. The radial wells enlarge the dewatering zone and enhance drainage ability. The electroosmosis wells are usually used in clay soil. In electroosmosis dewatering method, the voltage causes the negatively charged soil particles to move towards the anode, while the positively charged pore water is concentrated towards the cathode. Zheng et al. [10] presented the relationship between soil properties and electroosmosis reinforcement mechanics, which is caused by water drainage. However, light well point method has shown better effects in treating complex situation such as water in weakly permeable layer, which has been widely used in foundation pit engineering and foundation treatment. Some scholars have carried out experimental and in situ detection study on the light well point [11–13] to learn the transmission law of vacuum pressure and seepage law of pore water [14–20]. Light well point method works as a vacuum pump pumping out the air in the

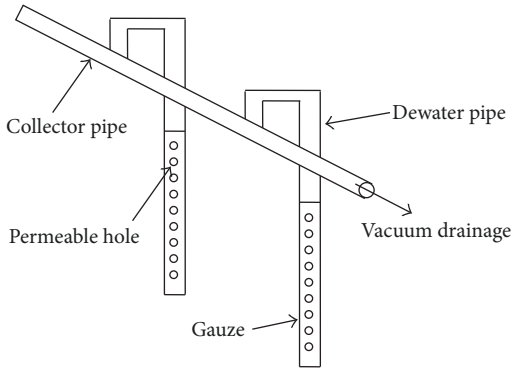

Figure 1: Diagram on light well point method.

well, the horizontal tube, and storage tank to form a negative pressure area in the soil. Meanwhile, the groundwater outside of the piping system is subject to atmospheric pressure and flows from the high pressure zone to the low pressure zone to maintain the equilibrium state. Groundwater is then pressed into the well and pumped away, which makes the water level drop. The diagram on light well point is shown in Figure 1. However, light well point works only on a shallow depth and small scale, which makes it not suitable for subway tunnel project with deep depth and large water flow. Therefore, tube well with large diameter combined with vacuum technique which is named vacuum tube dewatering method has been developed [21]. The diagram on vacuum tube well is shown in Figure 2.

Although the vacuum dewatering method has been widely used, its theoretical research is seriously inadequate. In particular, the groundwater level of vacuum dewatering is lack of research, which leads to the lack of theoretical basis for dewatering design. Nowadays, there is no theoretical equation to describe the water levels after vacuum dewatering, which leads to the vacuum dewatering wells that are designed according to the codes of nonvacuum wells and experiences in practice. The current methods make the predicted water levels after dewatering much higher than those in real situation because the effect of vacuum has not been considered. Therefore, this paper conducts theoretical and experimental research on the water level distribution under vacuum dewatering conditions and related laws, which aims at providing theoretical reference for the application of vacuum dewatering.

2. Vacuum Pressure Distribution in Soil and Waterhead of Vacuum Dewatering

In order to analyze the distribution of groundwater level under the effect of vacuum pressure, the distribution of vacuum pressure in soil should be studied firstly. It is known that, in practical engineering, the vacuum pumps always work for a long time. Therefore, it can be assumed that the air in the soil is in a state of steady seepage when it moves to the vacuum well and it follows Darcy's law because of the low velocity.

The model of soil particles and pores at a certain section, S, is shown in Figure 3.

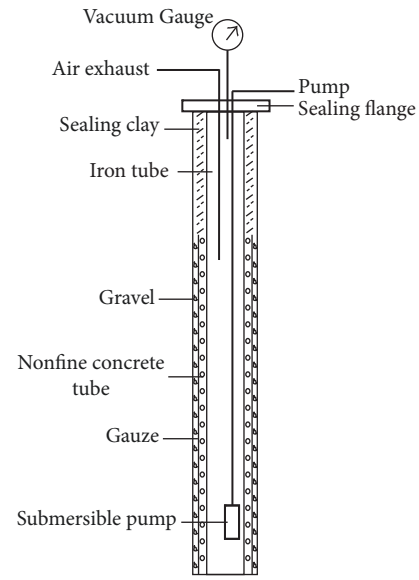

Figure 2: Diagram on vacuum tube dewatering method.

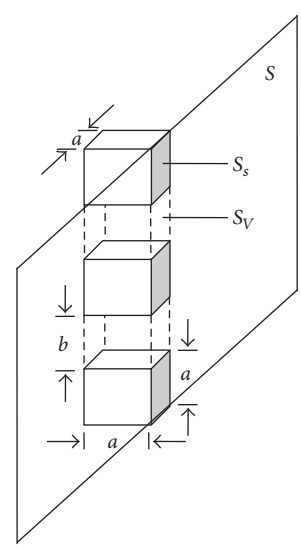

Figure 3: Soil particles and pores model.

In Figure 3, S_s represents the area of one side of cubic particle model and a is the side length of the model. S_V represents the area of one side of pore model while b is the distance of the adjacent particles.

The porosity ratio n can be derived from the model as follows:

$$n = \frac{a^2 b}{a^2 (a+b)} = \frac{b}{(a+b)}. \quad (1)$$

The ratio n_s of the cross-sectional area S is

$$n_s = \frac{S_V}{S_V + S_s} = \frac{ab}{a(a+b)} = \frac{b}{(a+b)}. \quad (2)$$

According to (1) and (2), $n = n_s$. Therefore, the porosity ratio of soil can be used to represent the porosity ratio at a

section. The velocity of the air passing through a section of soil can be expressed as

$$v = \frac{1}{r}\frac{q}{2\pi hn}. \tag{3}$$

According to Darcy's law,

$$\frac{dp}{dr} = \frac{v}{k_g} = \frac{1}{k_g}\frac{q}{2\pi rhn}. \tag{4}$$

Suppose $(1/k_g)(q/2\pi hn) = C$.

For a single layer of homogeneous porous media, the steady-state seepage control equation can be expressed as

$$dp = C\frac{1}{r}dr. \tag{5}$$

Equation (5) can be worked out as

$$p = CC_1 \ln r + C_2. \tag{6}$$

In order to solve (6), the boundary conditions are set to be

$$\begin{aligned} r &= r_r, \\ p &= p_r, \\ r &= r_w, \\ p &= p_w, \end{aligned} \tag{7}$$

where r_r is the distance from the vacuum well, p_r is the air pressure at r_r, and the pressure of the vacuum well with a radius of r_w is p_w.

Then

$$\begin{aligned} p_w &= CC_1 \ln r_w + C_2, \\ p_r &= CC_1 \ln r_r + C_2. \end{aligned} \tag{8}$$

In the end, the air pressure p in the distance of r from the vacuum well is worked out as in the following equation:

$$p = \frac{p_w - p_r}{\ln\left(r_w/r_r\right)} \ln\left(\frac{r}{r_w}\right) + p_w. \tag{9}$$

It is known that the 101 kPa air pressure (atmospheric pressure) can support waterhead of about 10.3 m [22], so the vacuum-induced head reduction Δh can be derived from the relation between atmospheric pressure and waterhead:

$$\Delta h = \frac{p_0 - p_w}{9806} - \frac{\left(p_w - p_r\right)\ln\left(r/r_w\right)}{9806\ln\left(r_w/r_r\right)}. \tag{10}$$

According to the Dupuit equation, the water level at the distance r from the dewatering well is

$$h_{\text{phreatic}} = \sqrt{h_w^2 + \left(H_0^2 - h_w^2\right)\frac{\ln\left(r/r_w\right)}{\ln\left(R/r_w\right)}}, \tag{11}$$

where h_{phreatic} is the waterhead within the influence radius of dewatering in phreatic water layer; h_w is the water level in the well; H_0 is the aquifer thickness; r is the distance between the measuring point and the center of the dewatering well; R is the influence radius of the dewatering.

In practice, the thickness of aquifer is uneven and generally thin. Therefore, it is assumed that the influence distance of the vacuum air pressure is longer than that of the dewatering. Then the waterhead under the effect of vacuum can be obtained when $R < r_I$:

$$\begin{aligned} h_{\text{phreatic-vac}} = {} & \sqrt{h_w^2 + \left(H_0^2 - h_w^2\right)\frac{\ln\left(r/r_w\right)}{\ln\left(R/r_w\right)}} \\ & + \frac{\left(p_w - p_r\right)\ln\left(r/r_w\right)}{9806\ln\left(r_w/r_r\right)} - \frac{p_0 - p_w}{9806}. \end{aligned} \tag{12}$$

Then the hydraulic gradient can be derived as

$$\begin{aligned} i_{\text{vac}} &= \frac{dh_{\text{phreatic-vac}}}{dr} \\ &= \frac{\left(H_0^2 - h_w^2\right)}{2r\ln\left(R/r_w\right)\sqrt{h_w^2 + \left(H_0^2 - h_w^2\right)\left(\ln\left(r/r_w\right)/\ln\left(R/r_w\right)\right)}} \\ &\quad + \frac{\left(p_w - p_r\right)}{9806r\ln\left(r_w/r_r\right)}. \end{aligned} \tag{13}$$

According to the flow formula,

$$Q = 2\pi rhki, \tag{14}$$

where Q is the volume of water, h is the water level, and k is the permeability coefficient.

Substituting (12) to i in (14), the value of Q under the vacuum effect will be

$$Q_{\text{vac}} = 2\pi rkh_{\text{vac}}\frac{dh_{\text{phreatic-vac}}}{dr}, \tag{15}$$

where h_{vac} is the water level under the effect of vacuum pressure.

At the same distance r, the value of Q without vacuum is

$$Q = 2\pi rkh_{\text{phreatic}}\frac{dh_{\text{phreatic}}}{dr}, \tag{16}$$

where

$$\begin{aligned} i_{\text{phreatic}} &= \frac{dh_{\text{phreatic}}}{dr} \\ &= \frac{\left(H_0^2 - h_w^2\right)}{2r\ln\left(R/r_w\right)\sqrt{h_w^2 + \left(H_0^2 - h_w^2\right)\left(\ln\left(r/r_w\right)/\ln\left(R/r_w\right)\right)}}. \end{aligned} \tag{17}$$

2.1. The Distribution of Water Level in Flow Boundary Conditions. When the flow at the boundary is the same, which means $Q_{\text{vac}} = Q$, the amount of pumped water in vacuum dewatering is the same as that in nonvacuum dewatering. The relationship of water level in vacuum and nonvacuum dewatering method is shown in the following equation:

$$\frac{h_{\text{phreatic}}}{h_{\text{vac}}} = \frac{dh_{\text{phreatic-vac}}/dr}{dh_{\text{phreatic}}/dr} = 1 + \frac{(p_w - p_r)\ln(R/r_w)\sqrt{h_w^2 + (H_0^2 - h_w^2)(\ln(r/r_w)/\ln(R/r_w))}}{4903\ln(r_w/r_r)(H_0^2 - h_w^2)}. \quad (18)$$

Then the water level of vacuum dewatering method is

$$h_{\text{vac}} = \frac{h_{\text{phreatic}}}{\left[1 + (p_w - p_r)\ln(R/r_w)\sqrt{h_w^2 + (H_0^2 - h_w^2)(\ln(r/r_w)/\ln(R/r_w))}/4903\ln(r_w/r_r)(H_0^2 - h_w^2)\right]}. \quad (19)$$

2.2. The Distribution of Water Level in Waterhead Boundary Conditions. It is assumed that the waterhead is constant at the boundary. Because the influence radius of the vacuum pressure is greater than the influence radius of dewatering ($r_I > R$), the water level in vacuum dewatering is worked out as follows:

$$h_{\text{phreatic-vac}} = H_0 - \frac{p_0 - p_w}{9806} + \frac{(p_w - p_r)\ln(r/r_w)}{9806\ln(r_w/r_r)}. \quad (20)$$

When r_r is equal to r_I, $p_r = p_0$. At the same time, it is found that when $h_{\text{phreatic-vac}} = H_0$, $r = r_r$. It can be seen that the influence radius of vacuum dewatering is the same as the influence radius of vacuum pressure. According to the Dupuit formula, the distribution of phreatic water level is determined by the boundary water level. So the boundary conditions are $r = r_w$, $h = h_w$; $r = r_I$, $h = H_0$. The distribution of phreatic water level can be obtained by substituting boundary conditions into the Dupuit formula:

$$h_{\text{phreatic-vac}} = \sqrt{h_w^2 + (H_0^2 - h_w^2)\frac{\ln(r/r_w)}{\ln(r_I/r_w)}}. \quad (21)$$

3. The Laboratory Experiment of Dewatering

It is concluded from theoretical analysis that the distribution of groundwater level will be affected by vacuum pressure, aquifer thickness, and other factors. In order to verify the theoretical formulas of groundwater level distribution of vacuum dewatering, the laboratory experiments of dewatering were carried out.

3.1. Experimental Equipment. The experimental system in ⌈ cludes model box, monitoring system, and vacuum generating system. The experimental system is shown in Figures 4 and 5.

3.1.1. Model Box. The model box is made of stainless steel. In order to make the model experiment close to the real vacuum dewatering, the upper and lower bottom surfaces of the box body are trapezoidal, and the model box is 100 cm in height and 200 cm in length. The width of pumping side is 5 cm and 20 cm in the water boundary side. The permeable steel plate is placed at the water boundary side to form a sink. At the end of the box, there are 4 waterhead control devices distributed at the height of 10 cm, 30 cm, 50 cm, and 70 cm, respectively. The nonwoven fabric is stuck to the permeable plate to prevent excessive soil particles from entering the sink and affecting the control of the hydraulic boundary conditions.

3.1.2. Monitoring System. The monitoring system includes water level and vacuum pressure monitor points. The water level monitoring pipes with the inner diameter of 8 mm are connected to the holes at the bottom of the box. The other ends are fixed on the board next to the model box. The lower edge of the board is 30 cm from the ground.

During the experiment, the influence range of vacuum was measured first at the vacuum monitoring points. The vacuum pressure gauges were placed at the corresponding points where the water level would be measured later. When the dewatering experiments started, the vacuum pressure gauges were removed and the soil surface was sealed by bentonite slurry.

3.1.3. Vacuum Generating System. The vacuum generating system consists of vacuum producing equipment and vacuum dewatering well. The dewatering well was made of PVC tube with inner diameter of 5 cm. The PVC tube was drilled with permeable holes with diameter of 5 mm. The permeable section of the well was 85 cm in height and was wrapped with 100 mesh nonwoven fabrics outside to prevent excessive fine particles entering the well. There was a sealing cover on the top of the well to keep the vacuum pressure in the well. The pumping pipe went through the sealing cover and the end of it was set to the needful depth.

The vacuum negative pressure was generated by an air compressor combined with a fluidic element. The vacuum pressure can be produced at different pressures by changing the pressure of air compressor.

3.2. Experimental Results and Discussion

3.2.1. Vacuum Pressure. In order to find out the influence range of the vacuum pressure, the distribution of vacuum pressure was measured firstly. The distribution of vacuum pressure is shown in Table 1 and Figure 6.

It is shown in Figure 6 that the influence distance of vacuum pressure was about 1.55 m when the vacuum pressure of dewatering well was about 2 kPa.

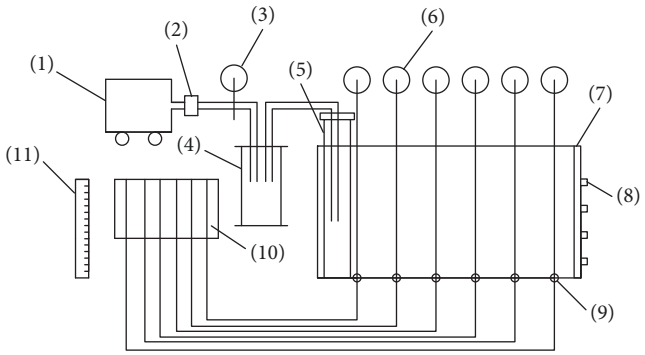

Figure 4: Schematic diagram of the experimental device. (1) Air compressor, (2) vacuum generator, (3) vacuum pressure gauge, (4) water separator, (5) dewatering well, (6) gauge, (7) water sink, (8) waterhead control, (9) pipes, (10) water level monitoring device, and (11) ruler.

Figure 5: Photograph of the experimental device.

Table 1: Distribution of vacuum pressure.

Distance to the well/m	0.05	0.35	0.65	0.95	1.25	1.55
Vacuum pressure/kPa	2	0.9	0.4	0.15	0.05	0

3.2.2. Water Level of Vacuum Dewatering and Nonvacuum Dewatering in Constant Flow Boundary Condition. The constant flow boundary condition was that the flow at the boundary remains the same. The specific parameters in the experiment are shown in Table 2.

At first, the waterhead on the injection side was kept at 0.7 m. And then, the injection flow q was set to 79 ml/min when pumping started. After the water level became stable, the water levels at each monitor point were recorded in both vacuum dewatering and nonvacuum dewatering tests.

Table 3 and Figure 7 present the water levels in theoretical calculation and experiment.

It is shown in Figure 7 that the experimental values of groundwater level were consistent with the variation trend of theoretical values. The theoretical and experimental water levels in both dewatering methods changed rapidly near the dewatering well and much slower in further distance. At the same time, the water level of vacuum dewatering method

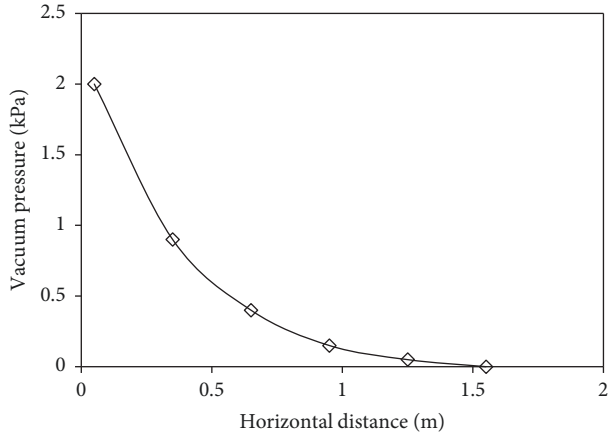

Figure 6: Distribution curve of vacuum pressure.

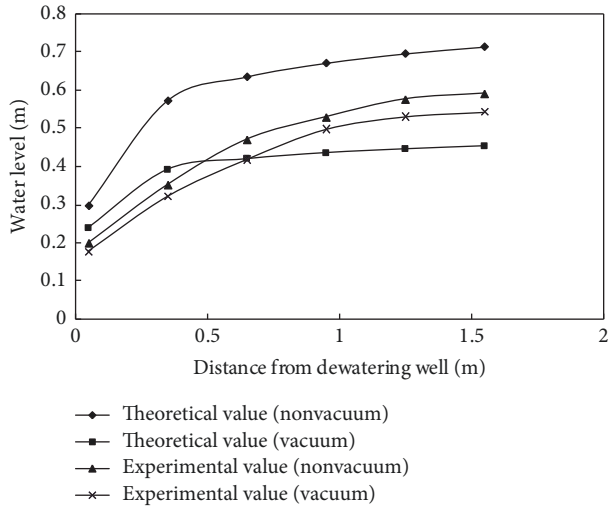

Figure 7: Water level in constant flow boundary condition.

is lower than that of nonvacuum dewatering method at the same distance, because a negative pressure zone was formed near the vacuum well and the hydraulic gradient has been increased. Due to the constant flow boundary condition, much more water could be drained off in vacuum dewatering than in nonvacuum dewatering method at the same time, which led to the lower water level in vacuum dewatering.

Therefore, it can be concluded that, under the constant flow boundary condition, the water level of vacuum dewatering is lower than the nonvacuum dewatering and the dewatering effect of vacuum dewatering is much better.

3.2.3. Water Level of Vacuum Dewatering and Nonvacuum Dewatering in Constant Waterhead Condition. The constant waterhead boundary condition was assumed that the waterhead at the boundary remained stable, which meant there was sufficient supply of water for the dewatering well. The parameters of soil and devices were the same as those in the constant flow boundary condition. Before starting the nonvacuum dewatering experiment, several conditions should be prepared. Firstly, saturate the soil in the model

Table 2: Specific parameters in experiment.

r_w (m)	h_w (m)	H_0 (m)	R (m)	r_r (m)	p_r (kPa)	p_w (kPa)
0.025	0.05	0.7	1.3	1.55	101	99

Table 3: Water level in constant flow boundary condition.

Distance from well (m)	Theoretical value of nonvacuum dewatering (m)	Theoretical value of vacuum dewatering (m)	Experimental value of nonvacuum dewatering (m)	Experimental value of vacuum dewatering (m)
0.05	0.297	0.24	0.199	0.177
0.35	0.573	0.393	0.352	0.321
0.65	0.636	0.421	0.471	0.418
0.95	0.672	0.437	0.53	0.497
1.25	0.697	0.447	0.577	0.53
1.55	0.715	0.455	0.592	0.542

Table 4: Water level in constant waterhead condition.

Distance from well (m)	Theoretical value of nonvacuum dewatering (m)	Theoretical value of vacuum dewatering (m)	Experimental value of nonvacuum dewatering (m)	Experimental value of vacuum dewatering (m)
0.05	0.579	0.578	0.554	0.552
0.35	0.654	0.65	0.6	0.58
0.65	0.676	0.671	0.64	0.622
0.95	0.689	0.684	0.665	0.65
1.25	0.699	0.693	0.682	0.673
1.55	0.706	0.7	0.694	0.686

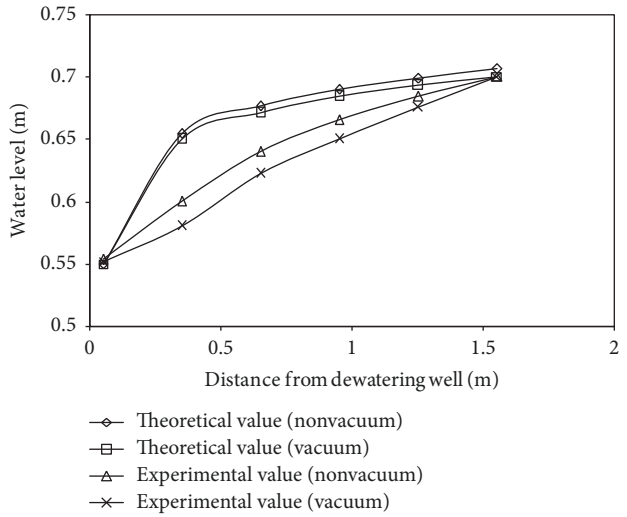

Figure 8: Water level in constant waterhead condition.

box and keep the water level at 0.7 m at the boundary sink. Secondly, the end of pump pipe in the well was laid at 0.55 m height from the bottom of the well. Thirdly, the water was drained off from the well and injected to the sink to keep the water level stay at 0.55 m in the well and 0.7 m at the sink. In order to ensure these conditions, the water pumping capacity should be much greater than the water supply at the boundary. Finally, the water level values at each monitoring point were recorded after the water level became stable. After finishing the nonvacuum dewatering experiment, the vacuum dewatering experiment was carried on by sealing the top of the well with other procedures as same as nonvacuum dewatering.

Table 4 and Figure 8 present the water levels in theoretical calculation and experiment.

It can be seen from Figure 8 that the theoretical values in vacuum dewatering and nonvacuum dewatering are larger than experimental values, but the variation trend of all curves in Figure 8 is almost the same. As in constant flow boundary condition, the water level in nonvacuum dewatering is lower than in nonvacuum dewatering method. However, the water level difference between vacuum dewatering and nonvacuum dewatering is smaller than that in constant flow boundary condition, because the boundary flow was fully supplied to keep the constant waterhead condition.

4. Conclusion

(1) The soil model including particles and pores was established and the vacuum pressure distribution was derived based on Darcy's law and steady-state seepage control equation.

(2) The boundary conditions of the seepage field were modified according to the vacuum pressure distribution law. Then the water level distribution of vacuum dewatering in constant flow boundary condition and constant waterhead condition was derived. In both boundary conditions, the water levels in vacuum dewatering were lower than in

nonvacuum dewatering, which showed the effectiveness of vacuum dewatering method.

(3) An indoor experiment has been carried out in order to analyze the water level distribution law in both dewatering methods and verify the theoretical model. As is shown in the experiment results, the theoretical values are consistent with the experimental values, which proves the rationality of theoretical equations and predicting the water levels in vacuum dewatering method. At the same time, the differences of water levels in waterhead boundary condition are smaller than those in constant flow boundary condition.

The derived theoretical model, which can be used for the reference of vacuum dewatering design, is suitable to predict the groundwater level distribution in vacuum dewatering according to the theoretical analysis and experiment.

Conflicts of Interest

The authors declare that they have no conflicts of interest.

Acknowledgments

This study is supported by the Fundamental Research Funds for the Central Universities of China (no. 2-9-2015-082).

References

[1] Y. Deva, H. Dayal, and A. Mehrotra, "Artesian blowout in a TBM driven water conductor tunnel in nortwest Himalaya, India," in *Proceedings of the 7th International IAEG Congress*, pp. 4347–4354, 1994.

[2] D.-J. Tseng, B.-R. Tsai, and L.-C. Chang, "A case study on ground treatment for a rock tunnel with high groundwater ingression in Taiwan," *Tunnelling and Underground Space Technology*, vol. 16, no. 3, pp. 175–183, 2001.

[3] S. Dalgi, "Tunneling in fault zones, Tuzla tunnel, Turkey," *Tunnelling and Underground Space Technology*, vol. 18, no. 5, pp. 453–465, 2003.

[4] Y. Shang, J. Xue, S. Wang, Z. Yang, and J. Yang, "A case history of Tunnel Boring Machine jamming in an inter-layer shear zone at the Yellow River Diversion Project in China," *Engineering Geology*, vol. 71, no. 3-4, pp. 199–211, 2004.

[5] J. Font-Capó, E. Vazquez-Suñé, J. Carrera, and I. Herms, "Groundwater characterization of a heterogeneous granitic rock massif for shallow tunneling," *Geologica Acta*, vol. 10, no. 4, pp. 395–408, 2012.

[6] D. Peila, F. Lombardi, and V. Manassero, "Stabilization of landslides using larger diameter wells , Landslides," in *Proceedings of the Landslides 6th International Symposium*, pp. 813–820, Balkema, Rotterdam, Netherlands, 1992.

[7] B. Bianco and D. A. Bruce, *Slope Stability Engineering Developments and Applications, Chapter 49*, The Institution of Civil Engineers, 1991.

[8] C.-S. Huang, S.-Y. Yang, and H.-D. Yeh, "Technical Note: Approximate solution of transient drawdown for constant-flux pumping at a partially penetrating well in a radial two-zone confined aquifer," *Hydrology and Earth System Sciences*, vol. 19, no. 6, pp. 2639–2647, 2015.

[9] M. Dimkic, V. Rankovic, N. Filipovic et al., "Modeling of radial well lateral screens using 1D finite elements," *Journal of Hydroinformatics*, vol. 15, no. 2, pp. 405–415, 2013.

[10] L. W. Zheng, X. Y. Xie, K. H. Xie, J. Z. Li, and Y. M. Liu, "Test and application research advance on foundation reinforcement by electro-osmosis method," *Journal of Zhejiang University (Engineering Science)*, vol. 51, no. 6, pp. 1064–1073, 2017.

[11] H. Yasuhara, M. Okamura, and Y. Kochi, "Experiments and predictions of soil desaturation by air-injection technique and the implications mediated by multiphase flow simulation," *Soils and Foundations*, vol. 48, no. 6, pp. 791–804, 2008.

[12] N. Li, X. D. Li, and Y. D. Wu, "Experiment study on the relationship between vacuum transfer law and permeability coefficient," *Subgrade Engineering*, vol. 4, pp. 101–103, 2011.

[13] F. Huang and G. Wang, "One-dimensional experimental research on vacuum degree transmission law in unsaturated soil," *Electronic Journal of Geotechnical Engineering*, vol. 17, pp. 3313–3322, 2012.

[14] J. C. Zhu, X. G. Wen, X. N. Gong, and Y. R. Cen, "Analysis of factors having effect on distribution of vacuum degrees during soft ground by vacuum drainage preloading," *Journal of Harbin Institute of Technology*, vol. 24, no. 4, pp. 603–605, 2003 (Chinese).

[15] J.-C. Chai and N. Miura, "Field vapor extraction test and long-term monitoring at a PCE contaminated site," *Journal of Hazardous Materials*, vol. 110, no. 1-3, pp. 85–92, 2004.

[16] L. H. Li, Q. Wang, N. X. Wang, and J. P. Wang, "Vacuum dewatering and horizontal drainage blankets: A method for layered soil reclamation," *Bulletin of Engineering Geology and the Environment*, vol. 68, no. 2, pp. 277–285, 2009.

[17] J. Saowapakpiboon, D. T. Bergado, P. Voottipruex, L. G. Lam, and K. Nakakuma, "PVD improvement combined with surcharge and vacuum preloading including simulations," *Geotextiles and Geomembranes*, vol. 29, no. 1, pp. 74–82, 2011.

[18] B. Indraratna, C. Rujikiatkamjorn, J. Ameratunga, and P. Boyle, "Performance and prediction of vacuum combined surcharge consolidation at Port of Brisbane," *Journal of Geotechnical and Geoenvironmental Engineering*, vol. 137, no. 11, pp. 1009–1018, 2011.

[19] B. Indraratna, C. Rujikiatkamjorn, A. S. Balasubramaniam, and G. McIntosh, "Soft ground improvement via vertical drains and vacuum assisted preloading," *Geotextiles and Geomembranes*, vol. 30, pp. 16–23, 2012.

[20] R. G. Robinson, B. Indraratna, and C. Rujikiatkamjorn, "Final state of soils under vacuum preloading," *Canadian Geotechnical Journal*, vol. 49, no. 6, pp. 729–739, 2012.

[21] X. M. Pan, *Research on Application of Compound Dewatering Technique of Vacuum Tube Well*, China University of Geosciences, Beijing, China, 2009.

[22] R. H. Charlier and J. R. Justus, *Ocean Energies: Environmental, Economic and Technological Aspects of Alternative Power Sources*, Elsevier, 1993.